



# HVOF-Sprayed Nano TiO<sub>2</sub>-HA Coatings Exhibiting Enhanced Biocompatibility

R.S. Lima, S. Dimitrievska, M.N. Bureau, B.R. Marple, A. Petit, F. Mwale, and J. Antoniou

(Submitted April 21, 2009; in revised form September 15, 2009)

Biomedical thermal spray coatings produced via high-velocity oxy-fuel (HVOF) from nanostructured titania (n-TiO<sub>2</sub>) and 10 wt.% hydroxyapatite (HA) (n-TiO<sub>2</sub>-10wt.%HA) powders have been engineered as possible future alternatives to HA coatings deposited via air plasma spray (APS). This approach was chosen due to (i) the stability of TiO<sub>2</sub> in the human body (i.e., no dissolution) and (ii) bond strength values on Ti-6Al-4V substrates more than two times higher than those of APS HA coatings. To explore the bioperformance of these novel materials and coatings, human mesenchymal stem cells (hMSCs) were cultured from 1 to 21 days on the surface of HVOF-sprayed n-TiO<sub>2</sub> and n-TiO<sub>2</sub>-10 wt.%HA coatings. APS HA coatings and uncoated Ti-6Al-4V substrates were employed as controls. The profiles of the hMSCs were evaluated for (i) cellular proliferation, (ii) biochemical analysis of alkaline phosphatase (ALP) activity, (iii) cytoskeleton organization (fluorescent/confocal microscopy), and (iv) cell/substrate interaction via scanning electron microscopy (SEM). The biochemical analysis indicated that the hMSCs cultured on n-TiO<sub>2</sub>-10 wt.%HA coatings exhibited superior levels of bioactivity than hMSCs cultured on APS HA and pure n-TiO<sub>2</sub> coatings. The cytoskeleton organization demonstrated a higher degree of cellular proliferation on the HVOF-sprayed n-TiO<sub>2</sub>-10wt.%HA coatings when compared to the control coatings. These results are considered promising for engineering improved performance in the next generation of thermally sprayed biomedical coatings.

**Keywords** biocompatibility, biomedical coating, human mesenchymal stem cells (hMSCs), HVOF spraying, implants, nanostructured TiO<sub>2</sub>

physiologic post-implantation stability, i.e., dissolution and osteolysis (pathologic process involving resorption of bone surrounding the implant) (Ref 2-4). Therefore, there is need to improve the performance of the current biomedical APS HA coatings.

## 1. Introduction

### 1.1 Hydroxyapatite Coatings

Hydroxyapatite (HA) coatings deposited via air plasma spray (APS) have been successfully employed as biomedical coatings for medical implants (e.g., load bearing bone implants such as hip-joints) (Ref 1). Despite the success of APS HA coatings, there are still concerns regarding their long-term performance related to the HAs

### 1.2 HVOF-sprayed n-TiO<sub>2</sub> as a Biomedical Coating

A possible alternative to improve the performance of APS HA coatings is based on the use of nanostructured titania (n-TiO<sub>2</sub>). Nanostructured agglomerated TiO<sub>2</sub> powders produced via spray-drying of individual n-TiO<sub>2</sub> particles have been thermally sprayed via the high-velocity oxy-fuel (HVOF) technique as an attempt to produce a new class of biomedical coating (Ref 5, 6). This coating was chosen due to the fact that it is a biocompatible material and it is not significantly absorbed/dissolved in the human body. In addition, it exhibits bond strength levels on Ti-6Al-4V substrates higher than 77 MPa (i.e., the epoxy glue breaks before the coating fails during the tensile adhesion test ASTM C633). Bond strength levels of APS HA coatings on Ti-6Al-4V substrates are normally below 30 MPa (Ref 5, 6). The high bond strength of these HVOF-sprayed n-TiO<sub>2</sub> coatings is of pivotal importance as the “relatively low” bond strength values of standard HA coatings in addition to resorption has led to late delamination and or debonding (Ref 2-4). In addition, previous preliminary studies demonstrated that the HVOF-sprayed n-TiO<sub>2</sub> coatings support fetal rat calvaria osteoblast cell growth and matrix production in levels equivalent to those of APS HA coatings (Ref 5, 6). In vivo experiments were also performed. Coatings were deposited

This article is an invited paper selected from presentations at the 2009 International Thermal Spray Conference and has been expanded from the original presentation. It is simultaneously published in *Expanding Thermal Spray Performance to New Markets and Applications: Proceedings of the 2009 International Thermal Spray Conference*, Las Vegas, Nevada, USA, May 4-7, 2009, Basil R. Marple, Margaret M. Hyland, Yuk-Chiu Lau, Chang-Jiu Li, Rogerio S. Lima, and Ghislain Montavon, Ed., ASM International, Materials Park, OH, 2009.

**R.S. Lima, S. Dimitrievska, M.N. Bureau, and B.R. Marple**, National Research Council of Canada, 75 de Mortagne Blvd., Boucherville, QC J4B 6Y4, Canada; and **A. Petit, F. Mwale, and J. Antoniou**, Lady Davis Institute for Medical Research, Jewish General Hospital, McGill University, 3755 Côte Ste-Catherine Road, Montreal, QC H3T 1E2, Canada. Contact e-mail: rogerio.lima@cnrc-nrc.gc.ca.



on small Ti-6Al-4V rods that were subsequently implanted in the femurs of rabbits. Grit-blasted Ti-6Al-4V rods without a coating were also implanted and served as a control. After 7 weeks of implantation, the rabbits were euthanized and the contact surface between the bone and implant was measured/evaluated via optical microscopy. On average, the contact surface between the HVOF-sprayed n-TiO<sub>2</sub> coating and bone was 1.7 times higher than that of the uncoated Ti-6Al-4V rods (Ref 5).

### 1.3 Enhanced Biocompatibility of Nanomaterials

Nanostructured zones were observed on the surface of the HVOF-sprayed n-TiO<sub>2</sub> coatings (Fig. 1). These zones were formed when semi-molten nanostructured agglomerated TiO<sub>2</sub> particles impinged and re-solidified on the previously deposited layers during thermal spraying (Ref 5, 6). The importance of the presence of nanozones on the coating surface comes from the widely accepted hypothesis that nanostructures enhance the biocompatibility of biomaterials (Ref 7). For example, nanozones may improve the adsorption of the adhesion proteins like vitronectin and fibronectin. These types of proteins mediate the adhesion of anchorage-dependent cells (such as osteoblasts) on substrates and coatings, as observed by Webster et al. (Ref 7) and Dalby et al. (Ref 8, 9). These adhesion proteins spread on the surface of an implant almost immediately upon its implantation in the human body. However, only a fraction of them stick or adsorb onto it. Shi et al. (Ref 10) and Lee et al. (Ref 11) observed that nano and submicron textured surfaces tend to exhibit a higher likelihood to retain proteins as a result of the interlocking between the proteins and nano-submicron asperities. When the osteoblast cells arrive at the implant surface they “see” a protein-covered surface that will connect with the transmembrane proteins (integrins) of the osteoblast cells, thereby promoting cell adhesion on the surface, as explained by Anselme (Ref 12). It should

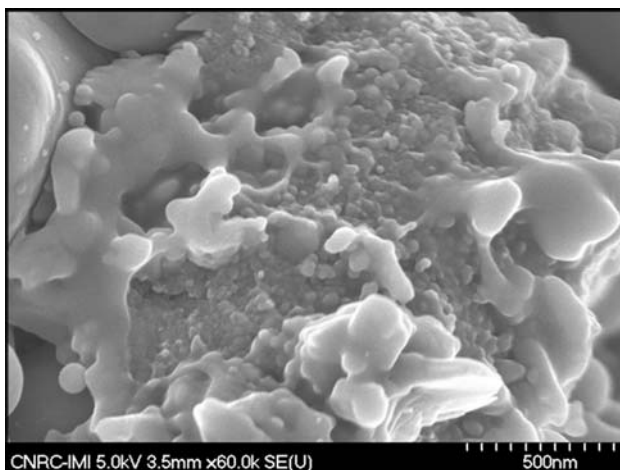


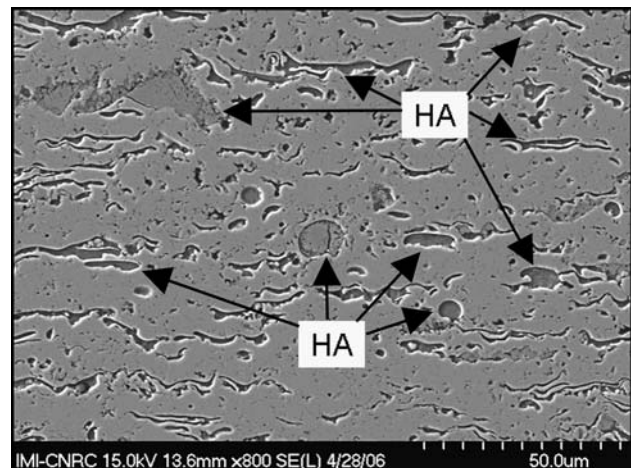
**Fig. 1** Nanostructured zone on the HVOF-sprayed n-TiO<sub>2</sub> coating surface (Ref 5)

be noted that these proteins, such as fibronectin, exhibit nanosized lengths and structures. For example, the average size of fibronectin is about 150 nm (Ref 13).

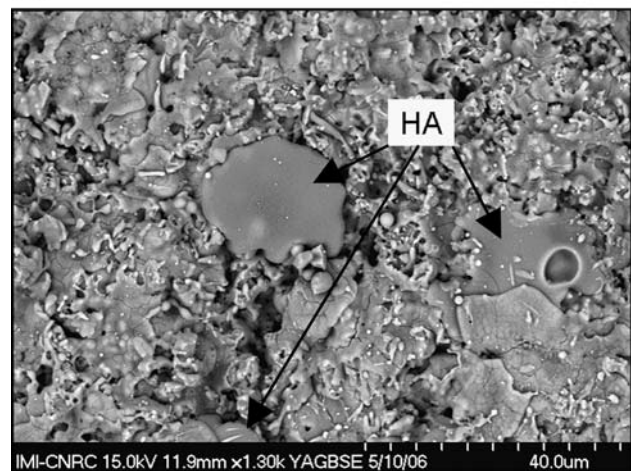
It is important to point out that Webster et al. (Ref 7, 14, 15) observed higher osteoblast proliferation levels on nanostructured ceramics (including TiO<sub>2</sub>) when compared to those of conventional ceramics. This higher osteoblast proliferation on nanostructured ceramics was attributed to the higher probability of protein adsorption caused by nano and submicron asperities on the nanomaterials' surfaces.

### 1.4 HVOF-Sprayed n-TiO<sub>2</sub>-10 wt.%HA Coatings

Based on these promising results, it was speculated that this “good” biological performance would be enhanced by adding HA on the coating structure. Therefore, n-TiO<sub>2</sub>-HA powder mixtures were produced and subsequently thermally sprayed via HVOF (Ref 16) (Fig. 2a, b). In spite of the HA addition, which is a weaker material, the bond



(a)



(b)

**Fig. 2** (a) Cross-section and (b) surface of an HVOF-sprayed n-TiO<sub>2</sub>-10wt.%HA (Ref 16)

strength levels were shown to be higher than 77 MPa for n-TiO<sub>2</sub>-10 wt.%HA coatings on Ti-6Al-4V substrates. Just like the HVOF-sprayed n-TiO<sub>2</sub> coatings, the epoxy glue was breaking before coating failure during the tensile adhesion test ASTM C633. It is important to point out that these HVOF-sprayed coatings exhibited porosity levels lower than 1% (Ref 16). Therefore, it is unlikely that the epoxy glue penetrated up to the coating/substrate interface, thereby affecting the bond strength data. As previously stated, bond strength levels of APS HA coatings are normally below 30 MPa (Ref 5, 6). These coatings have been engineered to exhibit nano and submicron structured surface texture (as those of the pure n-TiO<sub>2</sub> coating), in addition to the chemical character of HA, in an attempt to improve the coating biocompatibility. Therefore, it seems logical as the next step, to carry out biological experiments with these coatings.

### 1.5 The Interest on Human Mesenchymal Stem Cells

Currently, research works that have the goal of making stem cells to adhere on the surface of a scaffold or coated/uncoated substrate, and then grow to differentiate into specific cells are gaining importance, as pointed out by Olivier et al. (Ref 17), Zhang et al. (Ref 18), Sjöström et al. (Ref 19), and Kasten et al. (Ref 20).

The human mesenchymal stem cells (hMSCs) can be differentiated into a specific group of human cell types, e.g., osteoblasts (bone), chondrocytes (cartilage), myocytes (muscle), fibroblasts (connective tissue), and adipocytes (fat) (Ref 21). The use of hMSCs in the research and development of thermally sprayed biomedical coatings represents a very important alternative and a complement to the studies in which human osteoblasts cells are used (Ref 22). For example, once a prosthetic device (e.g., acetabular cup and femoral stem) is implanted in the human body, hMSCs produced by the bone marrow cover the surface of the implant. Once the hMSCs are well-adhered to the surface of the implant, they begin the process of proliferation and differentiation into osteoblast cells (Ref 21). Therefore, studying the behavior of hMSCs on the surface of these coatings provides important information and data about the onset of the interaction between the human cells and the implant, which affects both long-term biocompatibility and longevity of the implant.

It is important to point out the major difference between hMSCs and human embryonic stem cells (hESCs). The hESCs can be differentiated into any type of cell of the human body, whereas, as previously stated, hMSCs can differentiate into several but not all types of cells. However, hESCs are obtained from human embryos, which can lead to important ethical issues. hMSCs can be readily obtained from adult human bone marrow, which can be available during hip-joint replacement surgery, such as total hip replacement surgeries. This type of new data will provide valuable information to materials scientists, engineers, and biologists on how to engineer the next generation of high performance implants.

## 2. Experimental Procedure

### 2.1 Powders, Coatings, and Substrates for Thermal Spraying

The Ti-6Al-4V substrates employed in this work were cut into disk-shaped samples (pucks) of 12.7 mm diameter by 2 mm thickness. The substrates for coating deposition and control were grit-blasted with alumina grit #24, as a standard procedure of surface preparation (impurity removal and roughening) for thermal spraying. The average surface roughness ( $R_a$ ) was  $4.6 \pm 0.7 \mu\text{m}$  ( $n=10$ ). The thicknesses of all coatings varied from  $\sim 100$  to  $150 \mu\text{m}$ .

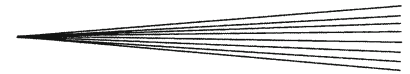
**2.1.1 n-TiO<sub>2</sub>.** The n-TiO<sub>2</sub> powder [VHP-DCS (5-20  $\mu\text{m}$ ), Altair Nanomaterials Inc., Reno, NV] was HVOF-sprayed (DJ2700-hybrid, Sulzer Metco, Westbury, NY) using propylene as fuel. The average particle temperature and velocity of the powder particles during the deposition step were  $1881 \pm 162 \text{ }^\circ\text{C}$  and  $686 \pm 93 \text{ m/s}$ , respectively. The average surface roughness ( $R_a$ ) of the coating was  $2.2 \pm 0.3 \mu\text{m}$  ( $n=10$ ). More details about this coating can be found elsewhere (Ref 5, 6).

**2.1.2 HA.** The HA powder (Captal 30 SD, Plasma Biotol, Tideswell, North Derbyshire, England) was pure and crystalline. It exhibited a nominal particle size of 15-50  $\mu\text{m}$ . This powder was sprayed via APS (SG100, Praxair, Concord, NH) using only Ar as plasma gas. The average particle temperature and velocity of the powder particles were  $2659 \pm 234 \text{ }^\circ\text{C}$  and  $189 \pm 19 \text{ m/s}$ , respectively. The coatings produced from this HA powder were used as a control. Crystalline HA and amorphous calcium phosphate were the main phases of the coating, with a minor content of tetracalcium phosphate. The average coating surface roughness ( $R_a$ ) was  $4.1 \pm 0.5 \mu\text{m}$  ( $n=10$ ). More details about this coating can be found in the paper of Auclair-Daigle et al. (Ref 23). The HA coatings were used as a control in this study.

**2.1.3 n-TiO<sub>2</sub>-10 wt.%HA.** The feedstock powder mixture was composed of 90 wt.%n-TiO<sub>2</sub>-10 wt.%HA. The starting n-TiO<sub>2</sub> and HA powders were the same materials employed for producing n-TiO<sub>2</sub> and HA coatings. The n-TiO<sub>2</sub>-10 wt.%HA powder was prepared through a mechanical-blending process in a planetary mill. This powder was HVOF-sprayed (DJ2700-hybrid, Sulzer Metco, Westbury, NY) using propylene as fuel. The average particle temperature and velocity of the powder particles were  $1875 \pm 162 \text{ }^\circ\text{C}$  and  $651 \pm 88 \text{ m/s}$ , respectively. The n-TiO<sub>2</sub>-10 wt.%HA coating exhibited rutile as major phase with anatase and HA as minor phases. No significant degradation of HA was observed by means of x-ray diffraction (XRD). The average coating surface roughness ( $R_a$ ) was  $3.0 \pm 0.5 \mu\text{m}$  ( $n=10$ ). More details about the coating can be found elsewhere (Ref 16).

### 2.2 Cell Isolation, Expansion, and Culture on Samples

**2.2.1 Human Mesenchymal Stem Cells.** Bone marrow samples were obtained from 15-mL aspirates from the



intramedullary canal of osteoarthritis patients undergoing total hip replacement surgery (three patients: 1 woman and 2 men, aged 52-76 years). Only tissue that would have been discarded was used, with the approval of the Research Ethics Committee of the Jewish General Hospital. This research also met the requirements of the ethics council committee of the National Research Council of Canada. The hMSCs were isolated and expanded as previously described (Ref 24). The medium was changed every 3 days, with all cultures maintained at 37 °C with 5% CO<sub>2</sub>. Culture-expanded hMSCs were trypsinized, counted, and seeded separately onto ethylene oxide (EtO) sterilized n-TiO<sub>2</sub>-10 wt.%HA, n-TiO<sub>2</sub>, and HA-coated pucks at a density of  $2 \times 10^4$  cells/cm<sup>2</sup>. Cells seeded on Ti-6Al-4V were used as references.

**2.2.2 hMSC Proliferation on Samples: Alamar Blue.** The n-TiO<sub>2</sub>-10 wt.%HA, n-TiO<sub>2</sub>, and HA-coated pucks seeded with the hMSCs were incubated for 1, 7, and 21 days. At each time point, the cell proliferation was monitored using the Alamar Blue™ assay according to the manufacturer (Biosource, Nivelles, Belgium). The assay is based on a fluorometric/colorimetric growth indicator that detects metabolic activity. Numerical data were analyzed statistically using independent Student *t*-tests.

**2.2.3 Biochemical Analysis: Alkaline Phosphatase Activity.** The alkaline phosphatase (ALP) activity of the conditioned media was evaluated as a determinant of osteoblast differentiation. The ALP activity, the driver of bone matrix mineralization, was determined in the hMSC lysates at 1, 7, and 21 days using a commercially available kit (AnaSpec, San Jose, CA) in accordance with the provided instructions. Briefly, the measurements were performed using 100 μL supernatants to which 100 μL of *p*-nitrophenolphosphate dye was added and the absorbance subsequently measured at 410 nm using a spectrophotometer. For each time point, the activities in three samples were normalized as μmol per mg protein per min.

**2.2.4 Cytoskeleton Organization (Confocal Microscopy): Immunocytochemistry (Fluorescence).** In order to visualize the cytoskeleton and nuclei of the hMSCs, after 1 and 7 days of hMSC seeding, two types of dyes were employed: propidium iodide (PI) for the nuclei and F-actin for the cytoskeleton. Briefly, cells were fixed in formaldehyde (Sigma, St. Louis, MO), permeabilized in 0.1% buffered Triton X-100 (Sigma, St. Louis, MO) and stained for cell cytoskeletal F-actin with 5 U/mL Alexa Fluor 488 phalloidin (Molecular Probes, Burlington, ON, Canada) for 1 h. Cell nuclei were counterstained with 15 M PI (Molecular Probes, Burlington, ON, Canada) for 20 min. Samples were mounted (Vectashield, Vector Laboratories, Burlington, ON, Canada) and examined optically (Cell Observer System, Carl Zeiss, Gottingen, Germany).

**2.2.5 hMSC/Substrate Interaction (SEM).** The morphologies of hMSCs were evaluated using a scanning electron microscope (SEM) (S-4700, Hitachi, Tokyo, Japan). The specimens were sputter coated with palladium and observed at 500× magnification.

## 3. Results and Discussion

### 3.1 Cell Proliferation

The Alamar Blue assay, which is based on the detection of metabolic activity of living cells, demonstrated that HVOF-sprayed n-TiO<sub>2</sub>-10 wt.%HA coatings supported the growth and proliferation of hMSCs (Fig. 3). The performance levels are equivalent or superior to those of standard APS HA coatings (Fig. 3) throughout the time of the study. It is important to point out that the hMSCs are anchorage-dependent cells, i.e., they will die if they do not become well-adhered to the surface of the coatings. Therefore, the results of Fig. 3 show strong evidence that the surface of the HVOF-sprayed n-TiO<sub>2</sub>-10 wt.%HA coating is creating favorable conditions for hMSCs adhesion, growth, and proliferation.

At this point, the dominant factor giving rise to the excellent behavior concerning the proliferation of hMSCs on the n-TiO<sub>2</sub>-10 wt.%HA coatings has not been precisely identified. However, some hypotheses can be examined. The observations of Shi et al. (10) and Lee et al. (Ref 11) on the effect of nano and submicron textured surfaces (like that of Fig. 1) on the likelihood of protein retention (interlocking), as well as the higher osteoblast proliferation on nanostructured ceramics observed by Webster et al. (Ref 7), should be taken into account in explaining the experimental results reported in this paper.

In addition, the overall surface roughness of the samples probably also played a role in these results. Comparing the information provided in Section 2, the HVOF-sprayed n-TiO<sub>2</sub>-10 wt.%HA exhibited roughness (*R<sub>a</sub>*) levels 27% lower than those of APS HA. This difference was caused mainly by the higher average velocity of the HVOF-sprayed particles when compared to that of APS HA particles (651 versus 189 m/s). Anselme et al. (Ref 25) evaluated the adhesion of human osteoblast cells on polished and sand-blasted Ti-6Al-4V surfaces. A higher degree of cell adhesion was observed on the polished surfaces. In this study, the uncoated Ti-6Al-4V substrates exhibited the highest roughness and the poorest performance of all samples tested (Fig. 3). Therefore, surfaces with lower degree of submicron and micron asperities (i.e., lower *R<sub>a</sub>* values) seem to facilitate hMSC adhesion.

It is important to point out that the addition of 10 wt.%HA to pure n-TiO<sub>2</sub> caused a noticeable improvement in the bioperformance of the n-TiO<sub>2</sub>-10 wt.%HA coating (Fig. 3). Consequently, not only the nano-micro topographical effects, but also chemical effects probably played an important role in the improved cell proliferation.

### 3.2 Biochemical Analysis

The early marker of osteoblastic activity measured in this study, ALP, demonstrated clear differences of cellular behavior among the different coatings (Fig. 4). At day 7, the activity of ALP levels were significantly higher in hMSCs plated on the n-TiO<sub>2</sub>-10 wt.%HA than in hMSCs plated on HA and n-TiO<sub>2</sub> reference coatings and on

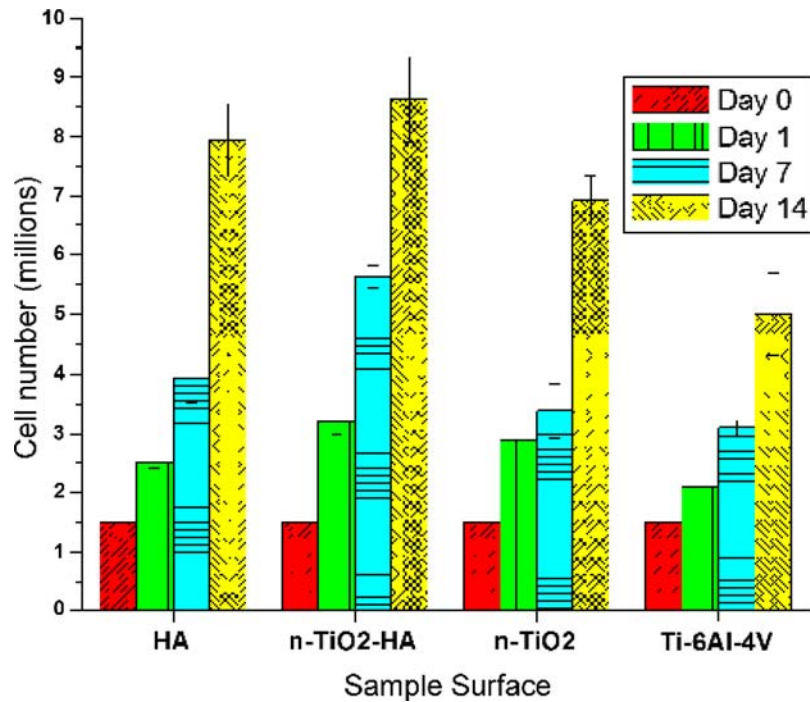


**Fig. 3** hMSC proliferation profiles during 14 days on HA, n-TiO<sub>2</sub>-10wt.%HA and n-TiO<sub>2</sub> coatings and uncoated Ti-6Al-4V substrates investigated by Alamar Blue

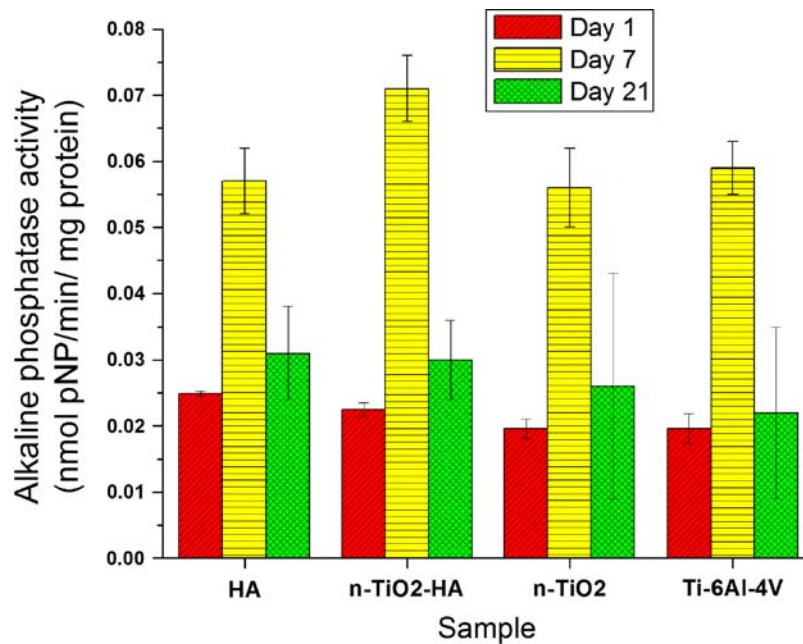


**Fig. 4** Normalized alkaline phosphatase activity (ALP), levels in medium of hMSCs cultured on HA, n-TiO<sub>2</sub>-10wt.%HA and n-TiO<sub>2</sub> coatings and uncoated Ti-6Al-4V substrates as a function of time

uncoated Ti-6Al-4V substrates. The increase in ALP activity is a marker of the commitment toward osteoblastic lineage, i.e., the trend of the hMSCs to differentiate into osteoblast cells. The significantly higher ALP increase on the n-TiO<sub>2</sub>-10 wt.%HA coatings symbolises the mesenchymal cells preference toward an osteoblastic lineage (bone building) when plated on n-TiO<sub>2</sub>-10 wt.%HA

coatings instead of the diametrically opposite possibility of osteoclasts (bone resorption) lineage.

### 3.3 Confocal Microscopy

Confocal microscopy in conjunction with fluorescence marking was used to investigate the cytoskeleton

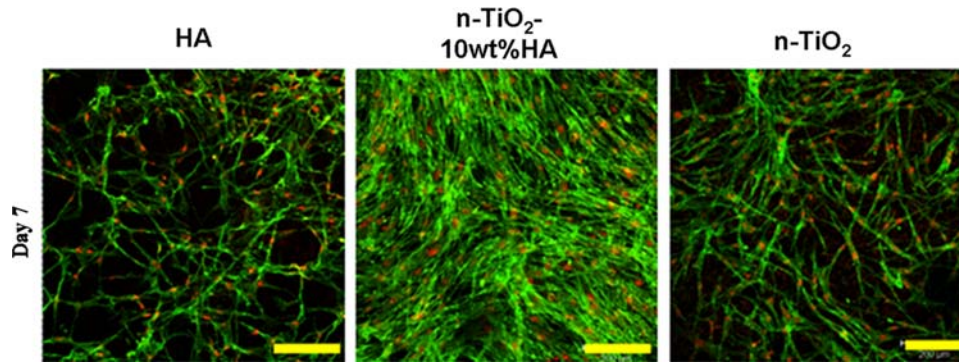
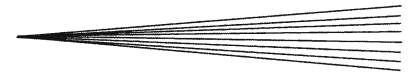
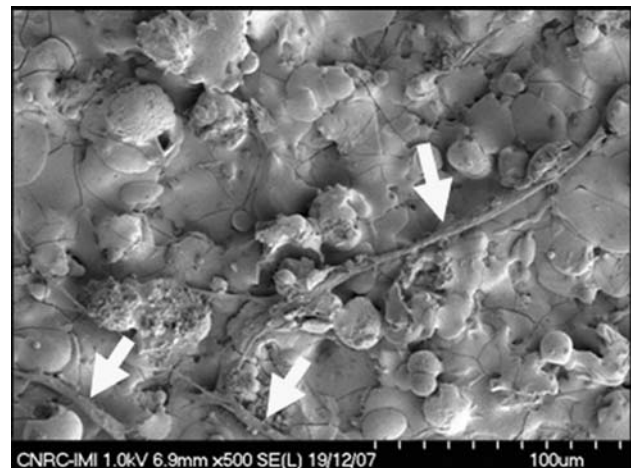


**Fig. 5** Cytoskeleton organization and nuclei morphology of hMSCs at day 7 cultured on HA, n-TiO<sub>2</sub>-10wt.%HA and n-TiO<sub>2</sub> coatings. The scale bar length is 200  $\mu$ m

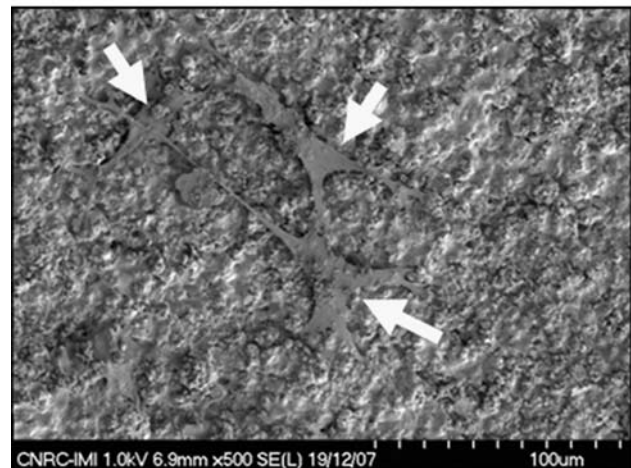
organization of the hMSCs at 7 days (Fig. 5). In addition, the nuclei staining technique was used to count the cellular number adhered to the various coating as a visual verification of the metabolic cellular proliferation. In Fig. 5, the nuclei are stained with PI (orange-red, disk-shaped) and the cytoskeleton with F-actin (green outline of the cellular body). The cellular growth kinetics among the hMSC plated on the APS HA, HVOF-sprayed n-TiO<sub>2</sub>-10 wt.%HA, and n-TiO<sub>2</sub> coatings are clearly visible. After 7 days of cell growth on the various surfaces, the hMSCs exhibited their typical growth phase: elongated or even spindle-shaped morphology similar on all three coatings. The visualization of cellular growth on all coatings confirmed the coatings anticipated biocompatibility. More importantly the F-actin filament deposition was clearly denser and more spread over the entire sample surface (and not only in areas of high cell density) of the HVOF-sprayed n-TiO<sub>2</sub>-10 wt.%HA coating when compared to the APS HA and HVOF-sprayed n-TiO<sub>2</sub> grown hMSC samples. Also, the number of cell nuclei (cell number), as can be visualized in Fig. 7, is significantly higher on the HVOF-sprayed n-TiO<sub>2</sub>-10 wt.%HA coating attesting to the previously seen increased growth kinetics on the n-TiO<sub>2</sub>-10 wt.%HA nanocomposites when compared to the reference coatings.

### 3.4 hMSC/Coating Interaction (SEM)

Figure 6 shows the SEM pictures regarding the interaction between the hMSCs and the coatings after 2 days of incubation. The hMSCs adhered, spread, and divided on the surface of all coatings. Particularly, at day 2 they exhibit the typical spindle hMSC shape and are elongated as previously seen in the fluorescence assay. Once again as with the fluorescence markings, the hMSC cultured on HA (Fig. 6a) seems to exhibit smaller cell bodies, limited spreading and more rounded morphologies when compared to the hMSCs cultured on n-TiO<sub>2</sub>-10 wt.%HA (Fig. 6b) and n-TiO<sub>2</sub> (not shown) coatings (the cells are highlighted by the arrows). This trend is important as cells in rounded configurations divide at a lower rates than those well flattened and spread on a surface, as previously shown by Hunter et al. (Ref 26). Therefore, the n-TiO<sub>2</sub>-10 wt.%HA (Fig. 6b) and n-TiO<sub>2</sub> (not shown) coatings seem to provide improved conditions for cell spreading,



(a)



(b)

**Fig. 6** hMSCs on the surface of the (a) APS HA and (b) HVOF-sprayed n-TiO<sub>2</sub>-10wt.%HA coatings after 2 days of cell culture—arrows highlight the cells

thereby enhancing their proliferation, as shown in the cell proliferation essays (Fig. 3 and 5). More information, further biomedical data and discussion on all the results of this paper can be found elsewhere (Ref 27).

### 3.5 Reaction between $\text{TiO}_2$ and HA at the Coating Microstructure

It can be hypothesized that a chemical reaction between  $\text{TiO}_2$  and HA may have occurred in benefit to the biocompatibility of the n- $\text{TiO}_2$ -10 wt.%HA system. Li et al. (Ref 28) deposited powder blends of HA+10 vol.% $\text{TiO}_2$  and HA+20 vol.% $\text{TiO}_2$  via HVOF. They have observed the presence of a  $\text{CaTiO}_3$  minor phase in the structure of the coatings by performing a regular XRD analysis. The XRD of the HVOF-sprayed n- $\text{TiO}_2$ -10 wt.%HA coating was previously analyzed (Ref 16); however, no other phases in addition to titania and HA were detected.

Coreño and Coreño (Ref 29) and Manso et al. (Ref 30) analysed the performance of  $\text{CaTiO}_3$  as an apatite growth promoter by using SBF. Both works reported promising results regarding the nucleation and growth of apatite. Consequently, if a similar type of event is occurring in the surface of the composite n- $\text{TiO}_2$ +HA coatings, it may be another factor that helps to explain the biological results of this paper.

Lu et al. (Ref 31) mechanically mixed HA and  $\text{TiO}_2$  powders and plasma-sprayed a blend of 50 vol.%HA+50 vol.% $\text{TiO}_2$ . The composite powder was sprayed into water. The powders sprayed into water were subsequently dried and evaluated via energy dispersive x-ray (EDX) analysis. No  $\text{CaTiO}_3$  phase formation was observed via XRD; however, the EDX analysis confirmed the presence of microregions with coexistence of Ca, P, and Ti in some melted particles, thereby indicating the inter-diffusion of elements from HA and  $\text{TiO}_2$ . Consequently, this type of reaction (i.e., inter-diffusion) may have occurred in the composite coatings produced for this study.

The same type of inter-diffusion observed when the powder was sprayed into water was also observed in the coating. The HA+ $\text{TiO}_2$  (50/50) composite powder was used to produce a bond coat (on a Ti substrate) for an HA topcoat. The composite coating exhibited similar

microstructure to that of the n- $\text{TiO}_2$ -HA coating of this work (i.e., a pile up of  $\text{TiO}_2$  and HA splats). Lu et al. (Ref 31) performed a linear EDX analysis at the HA and  $\text{TiO}_2$  splat interfaces. They also observed the coexistence of Ca, P, and Ti at those interfacial regions. Therefore, the same type of reaction between  $\text{TiO}_2$  and HA may have occurred in the coatings produced in this study.

To confirm this hypothesis, an EDX line scan analysis was performed at the upper layers of an HVOF-sprayed n- $\text{TiO}_2$ -10 wt.%HA coating (Fig. 7). It is possible to observe that for adjacent  $\text{TiO}_2$  and HA splats there are microregions containing the coexistence of Ti, Ca, and P atoms. Therefore, there is definitely an inter-diffusion among the elements of  $\text{TiO}_2$  and HA in the coating microstructure. However, as previously stated, the XRD spectrum of this coating did not detect any chemical reaction (e.g.,  $\text{CaTiO}_3$ ) between these two compositions (Ref 16). It was probably a sensitivity issue of the XRD analysis.

This chemical reaction between the  $\text{TiO}_2$  and HA and its effect on the biocompatibility of this coating will be one of the most important points to be sought in this ongoing work and presented in future publications.

## 4. Conclusions

Previous studies have shown that HVOF-sprayed n- $\text{TiO}_2$ -10 wt.%HA coatings exhibit bond strength levels higher than 77 MPa, i.e., at least twice those of APS HA coatings deposited on Ti-6Al-4V substrates, which are typically below 30 MPa. In addition, due to the high stability of  $\text{TiO}_2$  in the human body, longevity related concerns of HA coatings, such as, dissolution and osteolysis, are unlikely to occur. These results provide strong evidence that hMSCs exhibit on HVOF-sprayed n- $\text{TiO}_2$ -10 wt.%HA coatings (i) growth, proliferation, and attachment, (ii) commitment toward osteoblastic lineage, and (iii) cell/substrate interaction levels/characteristics

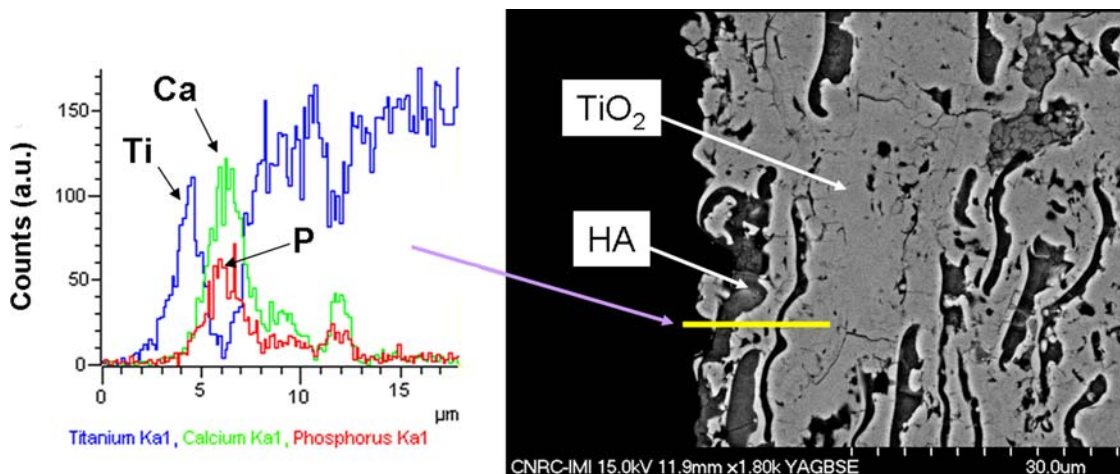


**Fig. 7** EDX line scan analysis at the upper layers of an HVOF-sprayed n- $\text{TiO}_2$ -10wt.%HA coating



superior to those of APS HA coatings. There are no clear explanations regarding this favorable behavior, but it is hypothesized that the nano-micro topography and chemical composition of the surface of the HVOF-sprayed n-TiO<sub>2</sub>-10 wt.%HA coating are playing important roles. The porosity distribution and residual stresses may also play a role. This is an ongoing work and these biocompatibility issues will be addressed in future publications. This results demonstrate that surfaces engineered in this fashion have the potential to become the next generation of biomedical thermal spray coatings with enhanced performance and improved longevity.

## References

1. L. Sun, C.C. Berndt, K.A. Gross, and A. Kucuk, Material Fundamentals and Clinical Performance of Plasma-Sprayed Hydroxyapatite Coatings: A Review, *J. Biomed. Mater. Res.*, 2001, **58S**, p 570-592
2. L.I. Havelin, B. Espehaug, and L.B. Engesaeter, The Performance of Two Hydroxyapatite-Coated Acetabular Cups Compared with Charnley Cups, *J. Bone Joint. Surg. (Br)*, 2002, **84-B**(6), p 839-845
3. O. Reikeras and R.B. Gunderson, Failure of HA Coating on a Gritblasted Acetabular Cup, *Acta. Orthop. Scand.*, 2002, **73**(1), p 104-108
4. K.A. Lai et al., Failure of Hydroxyapatite-Coated Acetabular Cups, *J. Bone Joint. Surg. (Br)*, 2002, **84-B**(5), p 641-646
5. R.S. Lima and B.R. Marple, Thermal Spray Coatings Engineered from Nanostructured Ceramic Agglomerated Powders for Structural, Thermal Barrier and Biomedical Applications, *J. Therm. Spray Technol.*, 2007, **16**(1), p 40-63
6. R.S. Lima and B.R. Marple, Engineering Nanostructured Thermal Spray Coatings for Biomedical Applications, *Bionanotechnology—Global Prospects*, D.E. Reisner, Ed., CRC Press/Taylor & Francis Group, Boca Raton, FL, Chap. 8, 2008, p 91-109
7. T.J. Webster, C. Ergun, R.H. Doremus, R.W. Siegel, and R. Bizios, Specific Proteins Mediate Enhanced Osteoblast Adhesion on Nanophase Ceramics, *J. Biomed. Mater. Res.*, 2000, **51**(3), p 475-483
8. M.J. Dalby, D. McCloy, M. Robertson, H. Agheli, D. Sutherland, S. Affrosman, and R.O.C. Oreffo, Osteoprogenitor Response to Semi-ordered and Random Nanotopographies, *Biomaterials*, 2006, **27**, p 2980-2987
9. M.J. Dalby, D. McCloy, M. Robertson, C.D.W. Wilkinson, and R.O.C. Oreffo, Osteoprogenitor Response to Defined Topographies with Nanoscale Depths, *Biomaterials*, 2006, **27**, p 1306-1315
10. H. Shi, W.-B. Tsai, M.D. Garrison, S. Ferrari, and B.D. Ratner, Template-Imprinted Nanostructured Surfaces for Protein Recognition, *Nature*, 1999, **398**, p 593-597
11. K.-B. Lee, S.-J. Park, C.A. Mirkin, J.C. Smith, and M. Mrksich, Protein Nanoarrays Generated by Dip-Pen Nanolithography, *Science*, 2002, **295**, p 1702-1705
12. K. Anselme, Osteoblast Adhesion on Biomaterials, *Biomaterials*, 2002, **23**, p 1187-1199
13. H.P. Erickson, N. Carrell, and J. McDonagh, Fibronectin Molecule Visualized in Electron Microscopy: A Long, Thin, Flexible Strand, *J. Cell Biol.*, 1981, **91**, p 673-678
14. T.J. Webster, R.W. Siegel, and R. Bizios, Osteoblast Adhesion on Nanophase Ceramics, *Biomaterials*, 1999, **20**, p 1221-1227
15. T.J. Webster, C. Ergun, R.H. Doremus, R.W. Siegel, and R. Bizios, Enhanced Functions of Osteoblasts on Nanophase Ceramics, *Biomaterials*, 2000, **21**, p 1803-1810
16. M. Gaona, R.S. Lima, and B.R. Marple, Nanostructured Titania/Hydroxyapatite Composite Coatings Deposited by High Velocity Oxy-Fuel (HVOF) Spraying, *Mater. Sci. Eng. A*, 2007, **458**, p 141-149
17. V. Olivier, N. Fauchoux, and P. Hardouin, Biomaterial Challenges and Approaches to Stem Cell Use in Bone Reconstructive Surgery, *Drug Discov. Today*, 2004, **9**(18), p 803-811
18. W. Zhang, X.F. Walboomers, T.H. van Kuppevelt, W.F. Daamen, Z. Bian, and J.A. Jansen, The Performance of Human Dental Pulp Stem Cells on Different Three-dimensional Scaffold Materials, *Biomaterials*, 2006, **27**, p 5658-5668
19. T. Sjöstrom, M.J. Dalby, A. Hart, R. Tare, R.O.C. Oreffo, and B. Su, Fabrication of Pillar-like Titania Nanostructures on Titanium and Their Interactions with Human Skeletal Stem Cells, *Acta Biomater.*, 2009, **5**, p 1433-1441
20. P. Kasten, I. Beyen, P. Niemeier, R. Luginbuhl, M. Bohner, and W. Richter, Porosity and Pore Size of  $\beta$ -tricalcium Phosphate Scaffold Can Influence Protein Production and Osteogenic Differentiation of Human Mesenchymal Stem Cells: An In Vitro and In Vivo Study, *Acta Biomater.*, 2008, **4**, p 1904-1915
21. M.J. Dalby, N. Gadegaard, R. Tare, A. Andar, M.O. Riehle, P. Herzyk, C.D.W. Wilkinson, and R.O.C. Oreffo, The Control of Human Mesenchymal Cell Differentiation Using Nanoscale Symmetry and Disorder, *Nat. Mater.*, 2007, **6**, p 997-1003
22. M. Sato, M.A. Sambito, A. Aslani, N.M. Kalkhoran, E.B. Slamovich, and T.J. Webster, Increased Osteoblast Functions on Undoped and Yttrium-doped Nanocrystalline Hydroxyapatite Coatings on Titanium, *Biomaterials*, 2006, **27**, p 2358-2369
23. C. Auclair-Daigle, M.N. Bureau, J.-G. Legoux, and L'H. Yahia, Bioactive Hydroxyapatite Coatings on Polymer Composites for Orthopedic Implants, *J. Biomed. Mater. Res.*, 2005, **73A**(4), p 398-408
24. D.C. Colter, R. Class, C.M. DiGirolamo, and D.J. Prockop, Rapid Expansion of Recycling Stem Cells in Cultures of Plastic-adherent Cells from Human Bone Marrow, *Proc. Natl. Acad. Sci. USA*, 2000, **97**, p 3213-3218
25. K. Anselme, M. Bigerelle, B. Noel, E. Dufresne, D. Judas, A. Iost, and P. Hardouin, Qualitative and Quantitative Study of Human Osteoblast Adhesion on Materials with Various Surface Roughnesses, *J. Biomed. Mater. Res.*, 2000, **49**(2), p 155-166
26. A. Hunter, C.W. Archer, P.S. Walker, and G.W. Blunn, Attachment and Proliferation of Osteoblasts and Fibroblasts on Biomaterials for Orthopaedic Use, *Biomaterials*, 1995, **16**, p 267-295
27. S. Dimitrievska, R.S. Lima, J. Antoniou, A. Petit, F. Mwale, M.N. Bureau, and B.R. Marple, TiO<sub>2</sub>-HA Nanocomposite Coatings Promote Human Mesenchymal Stem Cells Osteogenic Differentiation, *Biomaterials*, BIOMAT-S-09-02311
28. H. Li, K.A. Khor, and P. Cheang, Titanium Dioxide Reinforced Hydroxyapatite Coatings Deposited by High Velocity Oxy-fuel (HVOF) Spray, *Biomaterials*, 2002, **23**, p 85-91
29. J. Coreño and O. Coreño, Evaluation of Calcium Titanate as Apatite Growth Promoter, *J. Biomed. Mater. Res.*, 2005, **75A**(2), p 478-484
30. M. Manso, M. Langlet, and J.M. Martínez-Duart, Testing Sol-Gel CaTiO<sub>3</sub> Coatings for Biocompatible Applications, *Mater. Sci. Eng. C*, 2003, **23**, p 447-450
31. Y.-P. Lu, M.-S. Li, S.-T. Li, Z.-G. Wang, and R.-F. Zhu, Plasma-sprayed Hydroxyapatite+Titania Composite Bond Coat for Hydroxyapatite Coating on Titanium Substrate, *Biomaterials*, 2004, **25**, p 4393-4403